CHAPTER 7

EVENT-DRIVEN REAL-TIME PREDICTIVE VOLT/VAR OPTIMIZATION AND CONTROL

7.1 Introduction

Growth in installations of DERs is bringing unique opportunities and challenges to DNOs around the world. Therefore, advanced coordination and integration are essential for the efficient and reliable operation of future distribution systems. New technologies, such as AMI, ADMS include a suite of applications designed to monitor and control the entire distribution network in real-time [63], [97]. The integration of AMI on a large scale is enhancing the observability of ADN for real-time operations. The revised IEEE 1547 (2018) [89], also states that every DER must have reactive power support capability when requested by power system operators. Therefore, PV systems are increasingly being paired with smart inverters that can inject and absorb reactive power. Moreover, *the Smart Inverter Working Group Phase 3* has recommended eight functions to be included in *California Rule 21* as mandatory or optional for all inverter-based DER systems [90]. In order to do this, there is need of efficient fast real time controllers that can handle the undesirable issues smoothly. In this context, optimal Volt/VAR curve selection using a heuristics approach for VVC droop controller has been suggested in [7] and a gradient-based decentralized VVO approach under high DER penetration has been introduced in [8]. Though, real-time voltage and VAR regulation have been carried out in [64], [95], [100], [146], but few have analyzed CVR impact with VVC droop controllers.

This chapter presents an event-driven predictive control framework along with the local controller for CVR to maximize its benefits in terms of voltage reduction range and energy savings. In addition, the strategy addresses CVR adoption during sudden changes and limited voltage reduction issues. For local control, an autonomous VVC based droop controller is well known [21], [68], [77], [92], [111]. However, except [92] others has used the conventional droop method with predefined droop parameters. Under changing circumstances, the conventional VVC droop method may not be able to adopt the changes. Therefore, adaptive droop control has been introduced in this work. Moreover, event-driven co-simulation frameworks are suitable for real-time system operations as suggested in [154]–[159], hence this methodology has been adopted in this investigation for validation purpose. The contribution of the chapter includes:

- Event-driven predictive approach for real-time implementation of a multi-time scale, multi-objective VVC (MTMO-VVC) for aggregated and autonomous controls for ADN
- A coordinated three-layer hierarchical dispatching structure for the proposed event-driven predictive framework
- A communication free two-level adaptive droop based local controller for autonomous PV smart inverter operation
- The Development and validation of the proposed methodology in the real-time framework using the RTDS in distribution mode through co-simulation with models based on Python and OpenDSS models.

7.2 MTMO-Volt/VAR Control

A coordinated MTMO-VVC strategy for CVR, including multiple voltage control devices and the impact on the network devices and assets under different time scale, is presented in

this study. The detail description of the methodology is delineated in the below subsections.

7.2.1 Multi-Timescale Operation

The modern distribution system needs an operation in different time horizons under slow and fast timescales control. In daily operations, because of limited cycles and operational constraints, switched controls—such as OLTC, AVR, and capacitor banks—are rescheduled only a few times during the day. hence, slow-timescale control is sufficient for voltage support. However, a sudden change in the system and DER output might have detrimental effects on grid operations; hence, fast-response capabilities from inverters will play a vital role in handling the undesirable issues. Therefore, the proposed control strategy considers controls on both timescales (slow and fast). To do so, the entire time period is divided into Z slots for each day. For instance, if the value of Z is 24, then the duration of each slot of Z is 1 hour. Each slot is further sectionalized into *q* subslots indexed in minutes, with *dt* simulation time step in real-time, as shown in Figure 7.1. A detailed description of both timescales' operations is as follows.

7.2.1.1 STSC using Aggregated Approach

In order to coordinate and dispatch the VVO controller's set points for a finite period at feeder level, the aggregated control algorithm is adopted under STSC operation. VVO devices are scheduled in two sub-time intervals of i) minutes to hours and ii) minutes to seconds, as shown in Figure 7.1.

- *OLTC and Capacitor Banks: (Minutes to Hours):*

The OLTC and capacitor banks respond slowly. Moreover, limited cycles of operation and switching effects restrict the frequent operation of these devices. In practice, their operating range can usually vary from a few minutes to multiple hours; hence, in this study, the OLTC

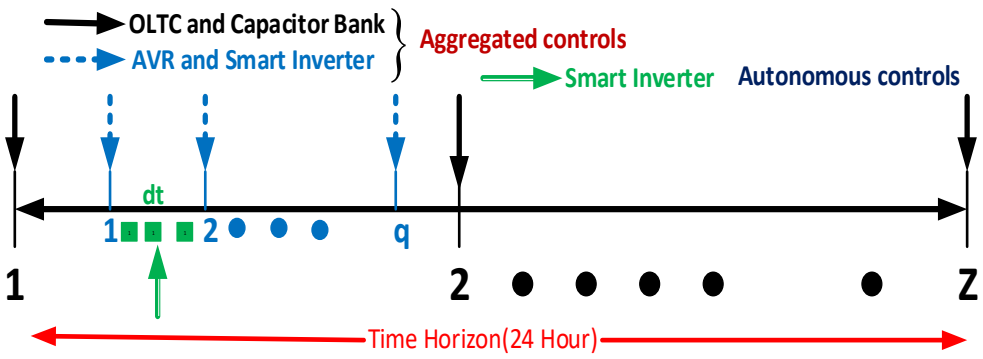

Figure 7.1. Multi-timescale horizon

and capacitor banks are scheduled for every 1-hour duration (as shown in Figure 7.1) during the entire day.

- *AVR and Smart Inverter: (Minutes to Seconds):*

Generally, voltage controllers such as AVR and smart inverters are scheduled for the duration of minutes to seconds. In this model, every 15 minutes, the setpoints of AVR and smart inverters are rescheduled; hence, shown in Figure 7.1, the value of q is set to 4 with the slot duration of 15 minutes.

7.2.1.2 FTSC using Autonomous Approach

In STSC operation, the VVO controllers are scheduled for a given time period. Under this time horizon (as set in STSC), however, there can be a deviation in DER output (such as PV active power) with respect to the forecasted value experienced. This happens due to intermittence behavior of solar PV power generations. Consequently, it might cause a detrimental impact on grid operations through violation of system limits such as voltage and power profile. Therefore, in this context, the fast-adaptive real-time control action is required to avoid such voltage limit violations. In order to do so, the fast-acting devices like smart inverters having the ability to respond quickly, and can absorb and inject reactive power are

utilized in this study. For this, an autonomous approach with adaptive two-level droop control has been proposed to regulate the inverter dispatch in a real-time framework.

7.2.2 Multi-Objective Control

In this study, multiple objectives are considered according to their timescale of operation. In the slow timescale, enabling of CVR through aggregated predictive VVO is the main objective. However, in the fast timescale, the goal is to control the voltage locally in real-time operation. To fulfill both objectives, the problem is combined to form a multi-objective control adopting the aggregated and autonomous approach simultaneously.

7.3 Event-Driven Predictive Framework

7.3.1 Overview of Event-Driven Predictive Approach

Figure 7.2 shows an overview of the event-driven predictive framework. This architecture has two data sources. The first has both forecasted data and historical event data from finished process instances.

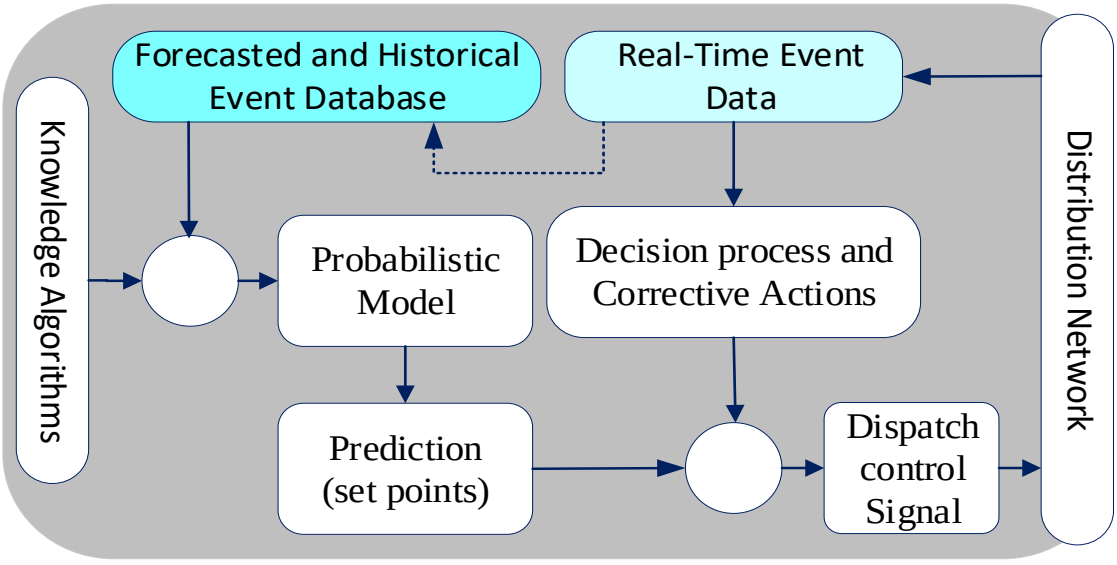

Figure 7.2. Schematic of an event-driven predictive framework

The real-time data from running process instances is another data source. After completion of the running process instance, the current event sequence added to the historical data. This study adopted a simple event log data format such as event log $Y = \{y^{(1)}, \dots, y^{(C)}\}$ having C as a sequence of events. Each event sequence $y^{(C)}$ is a tuple $\left(y_1^{(C)}, \dots, y_{t_c}^{(C)}\right)$ of t_c events where t_c is the length of event sequence $y^{(c)}$ [159]. Each event exclusively fits to an event type $y_t \in \{1 \dots . . E\}$ where E is the type of events. Approach commences with the selection of the suitable forecasted data (in this study loads and solar irradiation) subset for a given time scale. Afterward, the probabilistic model is fitted through a knowledge algorithm [159]. The solution obtained through a knowledge algorithm is used to generate the predictions (in this study controller's set points) and fed to the dispatch block where the control signal will be sent to the distribution network controllers. Afterward, real-time event data from the distribution network must be fed into the framework. A decision process block analyzes the measured sequence of events and sends corrective action to the dispatch block if required.

7.2.2 Probabilistic Model and Knowledge Algorithm

The probabilistic model-driven approach is a favorable scheme for handling the event-based predictive control problem in an optimal manner for a given prediction time horizon (Tp). In this context, probabilistic modeling powered by the knowledge algorithm has been adopted to achieve the sequence of optimal control setpoints and sent to the system to execute the control action during the control horizon 'Tc' ($Tc \leq Tp$). The main purpose of modeling the forecasted data probabilistically is to find a suitable representation that postulates the data into a probability distribution function over a given time framework. The present study considers the forecast data for load and solar PV power. To deal with the forecasting error, the proposed event-driven predictive methodology includes probabilistic modeling of the

uncertainty in the load and the solar PV irradiance predictions. The normal distribution method is used to generate uncertainty in the forecasted load data. On the other hand, the beta distribution is considered to model the PV irradiance uncertainty [30], [138].

Forecasted data of loads and solar irradiance for a given period have been fitted in normal and beta probabilistic distribution functions respectively, detailed explanations can be seen in previous *chapter 6*. A knowledge algorithm driven by monte-carlo sampling and simulation is used to generate number of scenarios (N) for solar irradiance and load consumption. A higher number of generated scenarios increases computation complexity and computational time. Hence, this study employed a K-means [148] clustering-based scenario reduction technique to reduce the number of scenarios (N') such that an accurate approximation of the system uncertainty should be maintained. After implementing the scenario reduction technique, the probability of the achieved scenarios is normalized (Ω_s^{norm}) as follows [138]

$$\Omega_{\mathrm{s}}^{\mathrm{norm}} = \frac{\text{Probability of occurance of one of reduced scenario}}{\text{Sum of the probability of occurrence of reduced scenarios}} \tag{7.1}$$

7.3.2.1 Objective Function: Stochastic Optimization

To maximize the energy savings, CVR has been formulated as a stochastic optimization problem with the objective of minimizing the sum of the square of the deviation of node voltages from the expected CVR voltage in all phases and all nodes except the source node for given *Tp* under slow time scale operation as shown in equation (7.2)

$$f = min \sum_{s=1}^{N'} \Omega_s^{norm} \sum_{t=\, t_k}^{t_k+\, T_p} \left[\left\{ \sum_{a,b,c} \sum_{i}^{l-1} \left(V_{i,h} - \, V_{CVR,h} \right)_{a,b,c}^{2} \right\} \right] \tag{7.2}$$

where $V_{i,h}$ is the node voltage (p.u.) at i^{th} bus at hour h; $V_{CVR,h}$ is the expected CVR voltage (p.u.) at hour h; *l* is the number of the nodes; and *a,b,c* are the phase notations.

7.3.2.2 Control Variables:

The taps of OLTC and AVR, reactive power dispatch of capacitor banks and smart inverters are the main decision control variables.

7.3.2.3 System Constraints:

The following operating constraints are subjected to equation (7.2)

- *Voltage Constraints:* Service voltage at the i^{th} load node must follow the relation as shown in equation (7.3):

$$0.95 \leq V_i \leq 1.05\ p.u. \quad (7.3)$$

- *Tap Constraint:* Tap of z^{th} OLTC/AVR (Tap_z) is given as

$$0.90 \leq Tap_z \leq 1.1\ p.u. \quad (7.4)$$

- *CB Constraints:* Reactive power supplied by j^{th} capacitor bank (Q_{CB}^{j}) is determined using equation (7.5):

$$Q_{CB}^{j} = W_{CB}^{j} \times \Delta q_{CB}^{j}, W_{CB}^{j} = \{0,1,2 \dots W_{CB}^{j,max}\} \quad (7.5)$$

where W_{CB}^{j}, Δq_{CB}^{j} and $W_{CB}^{j,max}$ are the number of switching steps, per step-change in Q_{CB}^{j} and available maximum number of switching steps at the j^{th} capacitor banks, respectively.

- *PV Smart Inverter (SI):* The reactive power dispatch of k^{th} PV inverter the in slow-timescale ($Q_{PV}^{k,stsc}$) is calculated by equation (7.6):

$$Q_{PV}^{k,stsc} = N_{PV}^{k} \times \Delta q_{PV}^{k}, N_{PV}^{k} = \{0,1,2 \dots N_{Pv}^{k,max}\} \quad (7.6)$$

where N_{PV}^{k}, Δq_{PV}^{k} and $N_{Pv}^{k,max}$ are the number of switching steps, per step-change in $Q_{PV}^{k,stsc}$, and available maximum number of switching steps at the k^{th} PV system, respectively. The maximum PV inverter reactive power $Q_{i,t}^{inv,max}$ is governed by the equation (7.7) where

$S_{PV_{inv}}^{k,max}$ and $P_{PV,t}^{k}$ are the PV inverter capacity and real power generation at instant t respectively.

$$\left|Q_{i,t}^{inv,max}\right| = \sqrt{\left(S_{PV_{inv}}^{k,max}\right)^2 + \left(P_{PV,t}^{k}\right)^2} \quad (7.7)$$

- *Voltage-Led Load Model:* The voltage-led composite ZIP (impedance current power) load model is considered for the study. The constant ZIP load model is shown in equations (1.17) -(1.20) respectively, as explained in *chapter 1*. This study uses the value of ZIP coefficients 0.36, 0.20, and 0.44 for both the active and reactive powers, respectively [160].

7.3.2.4 Solution Method:

The optimization problem defined in equation (7.2) is solved by DPSO followed by the system constraints. PSO is a population-based heuristic optimization technique [149]. It shares many similarities with evolutionary computation techniques. The particle dimensions are divided among decision variables. The optimization problem has been solved for the current prediction time horizon (T_P) based on predicted PV outputs and load demands, including forecasting errors. The achieved optimal day-ahead scheduling of control setpoints is dispatched to the VVO devices for the control horizon (T_C). The entire procedure is repeated when different observations come at t+1 for a complete day.

7.3.3 Decision Process and Online Corrective Action

After retrieving the real-time grid measurements both globally and locally, data is processed for event detections and take the corresponding decision for online corrective actions. The two-time scale window i.e. STSC in near real-time and FTSC in real-time has been intended to use for online operation. In near real-time, the corrective actions have been scheduled based on every fifteen minutes measured data set. Based on these global measures, the

decision has been processed weather the online corrective actions in current dispatches $X^o = \left[Tap_z, Q_{CB}^j, Q_{PV}^{k,stsc}\right]$ are required or not. In this context, Six sigma deployment based methodology has been adopted that comprises of five phases: define, measure, analyze, improve, and control (DMAIC) [161] for online process analytics and to determine the required corrective actions ($\Delta X^{corrective}$). The updated dispatches ($X^{updated}$) is calculated by equation (7.8)

$$X^{updated} = X^o \mp \Delta X^{corrective} \tag{7.8}$$

The detailed description regarding real-time control in fast time scale has been delineated below subsection.

7.3.4 Autonomous Approach for Real-Time Local Control

In a FTSC, the autonomous approach is best suited for controlling operation through smart inverter dispatches locally. The local controller dispatch reactive power based on local measurements to control the voltage fluctuations. For example, if $V_k(t)$ is voltage measurement at instant t, then corrective action is defined with relation (7.9)[156].

$$Q_k(t+1) = Ki\ (V_k(t)) \tag{7.9}$$

where $Q_k(t+1)$ is updated inverter Q dispatch for next *t+1* instant and *Ki*(.) is the local controller coefficient. To determine the appropriate value of $Q_k(t+1)$ in changing scenarios, the role of *Ki* is very important. Therefore, an adaptive droop-based local controller is deployed to enable the autonomous operation of the smart inverter to compensate the additional reactive power support. This additional VAR compensation would be additive to the optimal reactive power fed by PV inverters under aggregated STSC.

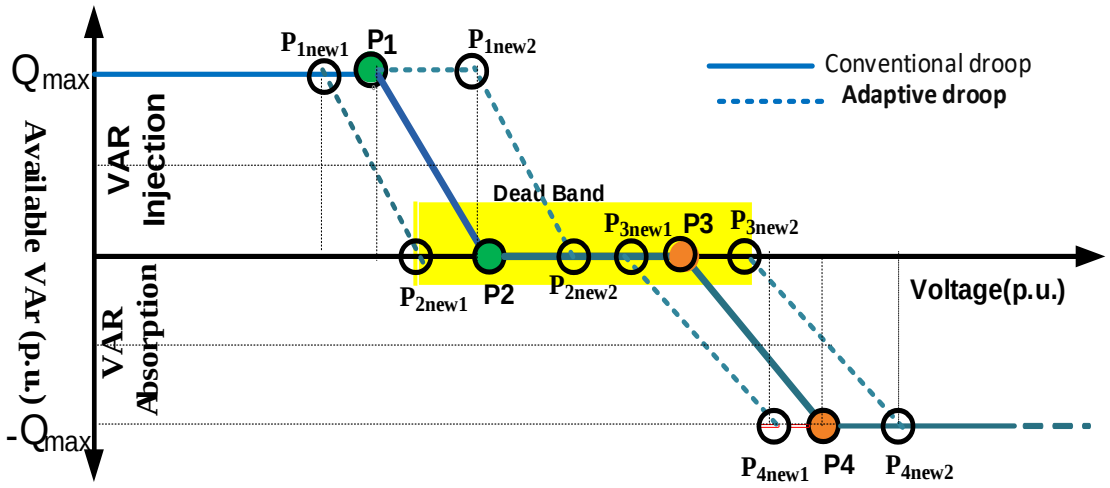

Figure 7.3. Adaptive Volt/VAR droop characteristics

7.3.4.1 Adaptive droop controller under FTSC

To determine the desired compensating reactive power from the PV system, the Volt/VAR droop characteristics are used for PV inverter VAR control. The adaptive Volt/VAR droop characteristics for the present problem are shown in Figure 7.3. The droop characteristic is obtained by defining the four-point (P1, P2, P3, and P4) parameters, also referred to as control/droop parameters. In conventional droop method, these parameters are constant or remain unchanged during the operation. However, these settings may or may not result the targeted output during changing operating conditions and external disturbance. Therefore, in this study adaptive droop controller has been introduced in which droop parameters are adopted according to the operating scenario. It can be seen from Figure 7.3 that the new droop parameters (P_{1new1}, P_{1new2}, P_{2new2}, P_{3new1}, P_{3new2}, P_{4new1} and P_{4new2}) are flexible and adaptive in nature using proposed control strategy. In order to do so, the two-level control approach has been utilized. In the first level, the droop controller uses pre-defined parameters and dispatches the control actions accordingly. Afterward, a correction factor (K_d) $= V_{specified} - V_{measured}$. based on local measurements has been calculated in order to check the voltage

limits and verify whether the correction in droop parameters is essential. If the K_d is outside the tolerance range, modification in the droop parameters is required. The second level deals with the selection of appropriate parameters utilizing K_d and steady-state error. The more details regarding steady state error and parameter selection can be found in [92]. The default droop parameters used in this study are depicted in Appendix C in Table C.3.

7.4 Real-time Co-Simulations Platform

The co-simulation platform has been made to examine the effect of different components, network assets and utility management applications involved in the operation and control of distribution grids. In order to do so; this study used the RTDS based co-simulation platform to check the effectiveness of the developed control algorithms including communication network delays.

7.4.1 Co- Simulations using RTDS -Python- OpenDSS

In this chapter, RTDS and OpenDSS have been utilized through Python in order to perform the real-time co-simulations. The generalized framework of the co-simulation platform has been shown in Figure 7.4. The detailed description regarding basic of RTDS has already been explained in *chapter 6* in subsection *6.7.3.1*.

To check the effectiveness of the developed control algorithms, a real-time a co-simulation platform is developed. In this context, a co-simulations framework through RTDS and OpenDSS with the help of external agents (such as Python for this study) has been introduced. This study uses RTDS Novacor, RSCAD 5.007 in *Distribution Mode* with simulation time step (dt) of 120 microseconds to test the developed control algorithms in a large-scale active distribution test system [150], [153]. The average models of PV DERs have been used.

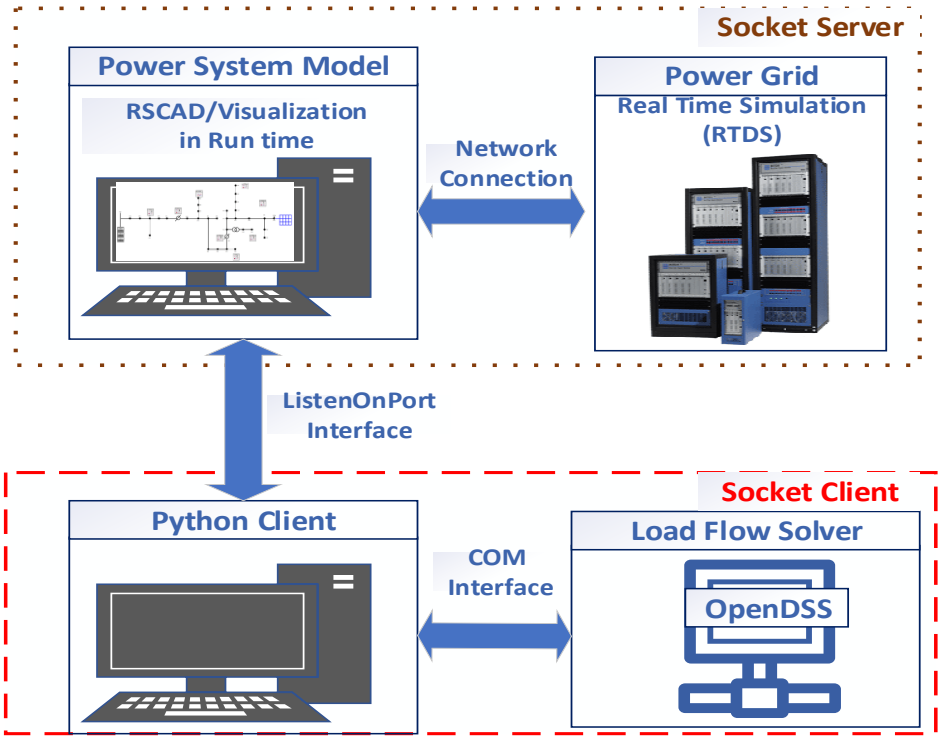

Figure 7.4 Framework of real-time co-simulation platform

The interaction during the real-time simulation in RTDS is implemented through '*ListenOnPort'* [150] command by external application, where the control algorithm was developed with the help of the OpenDSS platform.

7.4.2 Communication Interface

In order to interact with the simulation to external controllers or hardware, sometimes, the real-time simulation requires a standard communication protocol such as IEC-61850 and DNP 3 etc. In general, the specifications of these communication protocols are designed for a particular application. Besides, it is very hard to be modified frequently for the use of different purposes. Such specific use of communication protocols is also associated with the burden of the significant development in cost and effort. Moreover, some users who want to

send out the small set of control commands to the simulation and retrieve the corresponding measurements with lower interaction speed (usually in the range of hundreds of milliseconds) from external applications such as Python/ MATLAB [151]. Such needs can be fulfilled by a specific communication capability in RSCAD/Runtime through the scripting-based interface. The RTDS offer such a script-based '*ListenOnPort()*' command to enable the Transmission Control Protocol/Internet Protocol (TCP/IP) socket communication between RSCAD/Runtime and the applications running in the same network [150], [162]. The visualization of RTDS' output can be seen in its run time screen and it is in the same machine in which the RSCAD is installed, as shown in Figure 7.4. Once the connection established by execution of script commands the RSCAD/Runtime becomes a socket server and external application act as a socket client. This communication interface is generally known as socket communication.

7.4.3 Simulation Set up and Procedure

The interaction during real-time simulation in RTDS has intended through using '*ListenOnPort*' command by Python application where the control algorithm has been developed with the help of the OpenDSS platform as shown in Figure 7.4. The stepwise simulation procedure to interact with the RSCAD/Runtime server can be concise as follows [162].

- Once the '*ListenOnPort*' command is executed by the Runtime script reading engine, the RSCAD/Runtime becomes a specified port number.
- The external application, such as Python, executes the script and commences the essential client socket connection.

- The client application interacts with the Runtime TCP server port. Now, the socket communication is established.
- The socket communication is directed to the use of IP and TCP for address (AF INET) allocation and data streaming (SOCK STREAM) respectively.
- With the specifying of socket IP address and port number, the connection to the Runtime server is established. Now, the client (external application) can send commands to the run time simulations. These commands read as script commands by Runtime server.
- In order to ensure the synchronism between the Runtime and the external application Python (in this case) and also for bidirectional communications (i.e., from Runtime to the external application), a script command called '*ListenOnPortHandshake()*' can be used, It usage exchange of token string for synchronism acknowledgment. Meanwhile, that token string is also read the system measurements from RTDS simulation. A user-defined port is opened with TCP socket server.

7.5 Implementation of proposed methodology

The event-driven predictive control framework has been implemented using the developed real-time co-simulation framework as shown in Figure 7.4. A coordinated hierarchical dispatching structure [158] has been utilized for the execution of proposed methodology as described below subsection:

7.5.1 Coordinated three-layer hierarchical dispatching structure

The structure includes three layers for different timescales, such as scheduling, dispatching, and real-time control layer as shown in Figure 7.5. The control action is carried out in two modes of operation, as aggregated and autonomous controls, with different timescales. The scheduling layer works on a day-ahead hourly basis using a predictive control scheme to

obtain the VVO dispatches offline and stored in the sequence table. Besides, to limit the excessive tap excursion, a control strategy is adopted, as described in *Algorithm 1*. In the dispatching layer, if real-time measurements are violating the limits due to forecasting events error and inconsistency, the sequence table needs to be readjusted online based on current states. A control strategy as stated in *Algorithm 2*, is used to readjust the VVO dispatches and take online corrective action. The real-time control layer handles unpredictable violation events such as feeder voltage profile due to cloud transients and sudden change in network configuration and takes emergency action to eliminate such events immediately. In this context, a two-level adaptive droop-based autonomous real-time control for PV inverters are executed locally. A detailed procedure of the droop controller action is depicted in *Algorithm 3*. The overall implementation flowchart of the proposed methodology has been shown in Figure 7.6.

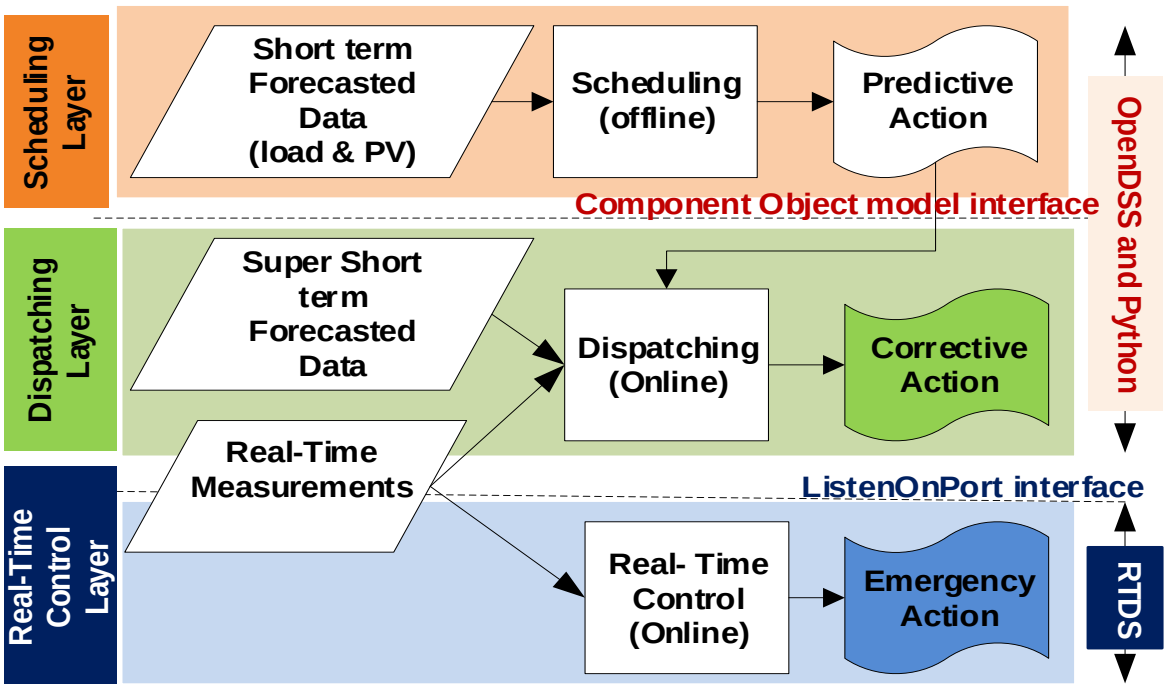

Figure 7.5 Coordinated three-layer hierarchical dispatching structure

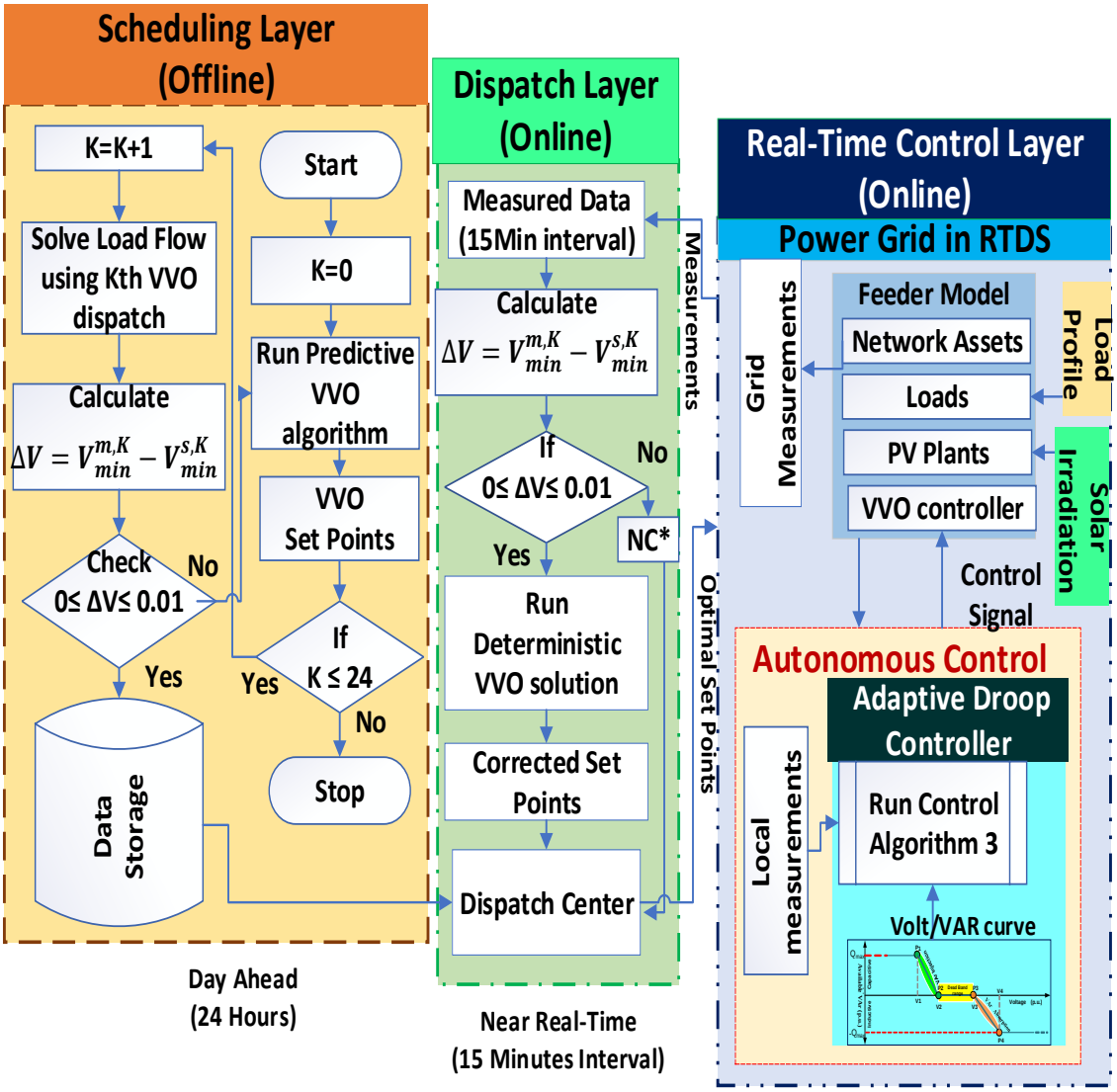

Figure 7.6. Implementation flowchart of the proposed methodology in real-time

(*NC – No change required. Already at optimal state, $V_{min}^{m,K}$, $V_{min}^{s,K}$ are the minimum measured and specified voltage, respectively)

The following special events type such as load and generation forecasting error event, voltage violation event, economic event (high power loss and CVR) and unpredicted events (cloud transients) have been considered to apply the proposed event-driven framework.

Algorithm 1: Predictive-driven day-ahead VVO scheduling layer (offline)

1 **Input:** Feed the required data of network assets and controllers
2 Initialize the counter K = 0
3 Run the predictive VVO algorithm using equation (7.2) subject to system constraints equations (7.3) -(7.8)
4 Obtain the current state VVO dispatch and stored in the sequence table
5 ***If*** K reaches its maximum limit (number of stages i.e. 96),
6 Then, stop the time series simulation
7 ***Else,*** set the counter K = K+1
8 ***Do*** the power flow using OpenDSS with previous K^{th} state
9 Then calculate: $\Delta V\ (p.u.) = V_{min}^{measured,K} - V_{min}^{specified,K}$
10 ***If*** $0 > \Delta V > 0.01$
11 Go to Step 3
12 ***Else,*** store the VVO dispatch in data storage
13 Repeat the entire process for the whole day
14 ***End***

Algorithm 2: Dispatching layer near real-time online control

1 **Input:** Feed the required load and PV solar irradiation data in the feeder model in a real-time digital simulator (RTDS)
2 Get the VVO schedule in the dispatch center from the scheduling layer
3 Send the setpoint commands to the real-time simulation
4 Collect the real-time measurements in each 15-minute interval
5 Calculate the correction factor
$\Delta V\ (p.u.) = V_{min}^{measured,K} - V_{min}^{specified,K}$
6 ***If*** $0 > \Delta V > 0.01$
7 Solve the deterministic VVO problem (7.2), subject to system constraints using Python- and OpenDSS-based co-simulations
8 Obtain the corrected dispatches, modify the sequence table
9 Send the corrected set points through the dispatch center
10 ***Else,*** no change is required; already in the optimal sate
11 ***End***

Algorithm 3: Two-level adaptive droop-based controller for Autonomous Controls operating in real-time control layer

Input: Feed the optimal VVC parameters for considered CVR duration obtained through *Algorithm 1*

Input: Feed the pre-defined droop characteristic parameters (P1, P2, P3, and P4 and deadband)

for time duration 0< t < T (as defined in STSC)

    If PV power output deviates from the forecasted value,

        check the voltage limits

        Else, if voltage profile is in the dead band range

            Control action: No action is required.

        Else, if voltage limit is violated

First Level control:

        Droop controller operates with pre-defined parameters

        Control action: Injects/absorb the compensated Q power

Second Level control:

            Calculate the correction factor (K_d)

            If , K_d is within tolerance range, no further action is required

            Else, calculate the new droop parameters using K_d

            Control action: Set the new droop parameters and injects/absorb the compensated Q power accordingly

        End

    End

End

Output: Desired additional reactive power compensation achieved.

7.6 Case study

7.6.1 Test System Description

To validate the proposed methodology, a modified IEEE 123-feeder test is considered, as shown in Figure 7.6 [24]. The total nominal load is 3.524 + j1.940 MVA, and the maximum

PV active power generation is 2.2 MW, with approximate 63% penetration. The three PV systems are connected to nodes 66abc (PV1), 26ac (PV2), and 104c (PV3) with the inverter ratings of 1,000 KVA, 800 KVA, and 400 KVA, respectively. Per-step reactive power variation from the PV inverter is 10 kVAR for the slow timescale. The OLTC and AVR transformers have ±16 taps with a per-step increment of 0.00625. The three-phase capacitor bank (CB 1) is connected to Node 83 having 200 kVAR per phase capacity with step variations from 0 to 4. Three single-phase capacitor banks (CB-2, CB-3, and CB-4) are connected to nodes 88a, 90b, and 92c, respectively, having a maximum rating of 50 kVAR. The hourly forecasted and real-time load demand and solar irradiation are shown in Figure 7.8 and Figure 7.9 for an entire typical day were taken from NREL's SMART-DS project. The controlling parameter used in the DPSO is depicted in Appendix C in Table C.1.

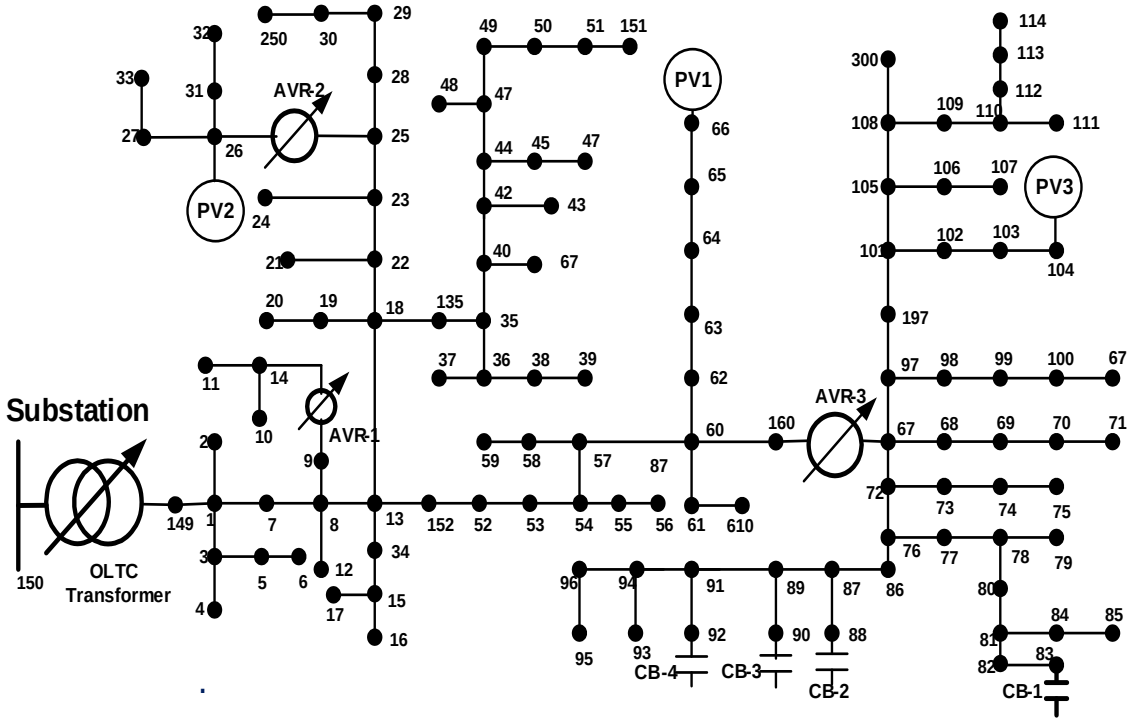

Figure 7.7 Modified IEEE 123-node distribution test feeder

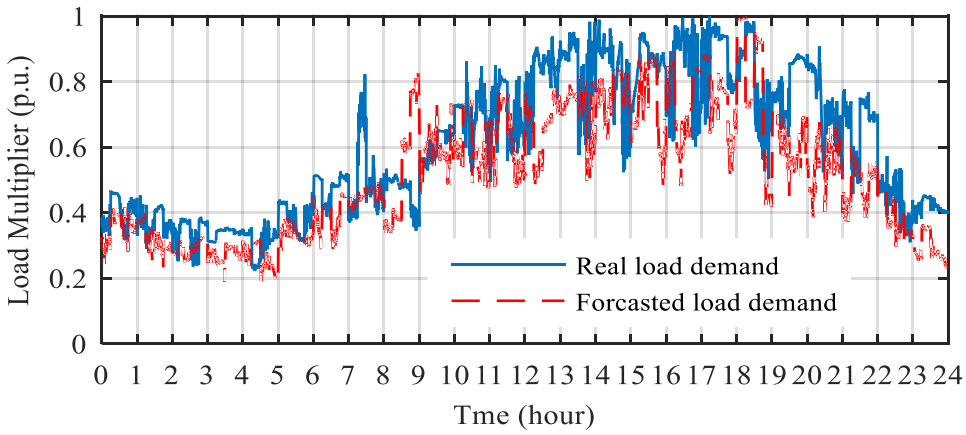

Figure 7.8. Real and forecasted load demand profile for a day

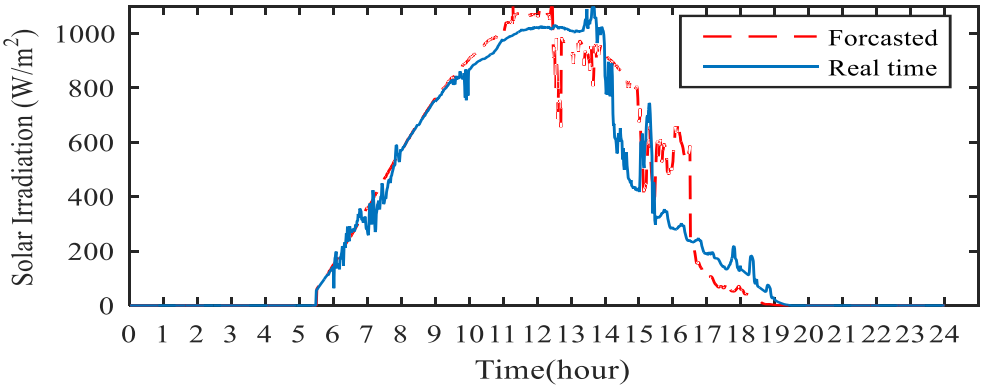

Figure 7.9. Real and forecasted solar irradiation profile for a day

7.6.2 Modes of VVC operation

The performance of the proposed method is validated for two different timescales (slow and fast) under the following three modes of VVC operation:

- *Mode 1: No CVR (Normal Operation):* In this mode, the system does not deploy CVR for VVC operation. The execution of VVC is carried out with OLTC, AVR-1, and AVR-2 at 120-V regulated voltage and AVR-3 at 124 V. Fixed CBs are used.
- *Mode 2: Traditional CVR:* In this mode, the LDC scheme is deployed for voltage reduction. The regulated voltages/end of the line are fixed in the lower half range (120 V–114 V) of

the service voltage. The control action is determined through the LDC algorithm. A detailed discussion of the LDC control mechanism is described in previous *chapter 2*. In the traditional method, the regulation voltage 118 V for OLTC, AVR-1, AVR-2, and AVR-3 is adopted to enable CVR. The level of voltage reduction can be increased to achieve increased energy savings; however, this might violate the minimum voltage limits at some points of the ADN.

- *Mode 3: Event-Driven Predictive VVO-Based CVR:* In this mode, the test system is simulated with the proposed event-driven predictive VVO-based CVR operation. The simulated results are described in Table 7.1. The event-driven predictive VVO predicts the solar PV irradiance and load demand for the next 1 hour in each 15-minute interval. Afterward, it determines and executes the control decisions for every 15-minute interval. Monte Carlo simulations are used to generate the 500 scenarios (N = 500) that signify the forecasted error in the prediction horizon. After that, the generated 500 scenarios are reduced to 15 scenarios (N' = 15). The stochastic VVO problem defined in equation (7.2) is solved every prediction horizon (1 h) using the DPSO technique.

7.6.3 Daily Energy Scheduling layer (offline simulations): Predictive Action

The proposed aggregated control *algorithm 1* is validated for the day-ahead scheduling in offline mode, considering the uncertainty in the network model. The test system is simulated for the modes, as mentioned. Table 7.1 shows the simulation results of all modes of operation. The Mode 1 (No CVR) operation results are depicted in the second column of Table 7.1. In Mode 2, CVR operation uses the traditional method, and results are portrayed in the third column of Table 7.1. Results show that around 3.96% of energy demand and 2.410% of energy losses are reduced during Mode 2 operation. Moreover, about 2.206% peak power

demand and 1.33% peak power loss are also decreased. Although sufficient energy savings and demand reduction can be achieved with traditional CVR (Mode 2), this scheme does not cooperate when any uncertainty is encountered in the network model. Moreover, system constraints are violated during deeper voltage reduction with improper VAR management. On the other hand, the proposed Mode 3 operation is capable of handling the network uncertainty, such as forecasting errors in load and generation, with proper coordination among multiple voltage regulation devices and network assets. Results shown in the fourth column of Table 7.1 indicate a reduction of about 5.039% daily energy demand and a decrease of about 4.337% kWh energy losses. AS shown by the simulation results depicted in Table 7.1, Mode 3 operation exhibits much more energy and power savings than Mode 1 and Mode 2 operations.

Table 7.1. Simulation results for the day-ahead Energy Scheduling

Energy (E)Terms	**Mode 1 (No CVR)**	**Mode 2 (Traditional CVR)**	**Mode 3 (Event-Driven Predictive-VVO-Based CVR)**
E_{demand} (MWh)	37.3005	35.8338	35.4210
ΔE_{saving} in MWh, (%)	----	1.4667, (3.96)	1.8796, (5.039)
E^{p}_{losses}, MWh	0.8055	0.7861	0.77061
ΔE^{p}_{losses} in kWh, (%)	----	19.420, (2.410)	34.937, (4.337)
Peak kW Demand	3166.60	3083.203	3044.55
ΔP_{saving} in kW, (%)	----	83.39381, (2.206)	122.0464, (3.85)
P_{losses}, kW	73.3667	72.5353	71.15977
ΔP_{losses} in kW, (%)	----	0.8315, (1.333)	2.2069, (3.08)

7.6.4 Online Real-Time Validation In RTDS

In this section, the proposed control algorithm is validated in the developed real-time co-simulation platform in online, as described in subsection 7.4. The 1-hour time duration from 14:00 to 15:00 is considered for the simulation period. The corresponding real-time load and solar irradiations are shown in Figure 7.8 and Figure 7 .9. The developed control *algorithms (2 and 3)* are tested in the STSC and FTSC scenarios, respectively.

7.6.4.1 Validation under STSC: Corrective Action:

The STSC operates in both hourly and 15-minute time intervals, as discussed in section 7.2. A near-real-time aggregated control scheme is best suited for this horizon, with the corrective action in each 15-minute interval, as shown in the flowchart in Figure 7.6 under the dispatching layer. The time-series simulations are carried out according to *Algorithm 2* for the considered time period using the developed co-simulation platform. The megawatt power demand without CVR and with proposed predictive VVO-based CVR and CVR saving is shown in Figure 7.10 and indicates that a significant amount of power demand reduction can be achieved with model predictive VVO-based CVR. Moreover, event-driven predictive VVO-based CVR reduces energy demand by about 5.39% during a 1-hour CVR duration. In addition, Table 7.2 shows the change in VVO set points during the CVR operation. Table 7.2 also shows that the action required from the OLTC and capacitor banks are in an hourly duration. On the other hand, AVR and smart inverter execute an optimal control action in a 15-minute interval according to the correction factor. If the correction factor is within limits, then no change is required. The setpoints are already at an optimal state. If not, calculate the corrected set points and corresponding required the number of changes, as shown in Table 7.2.

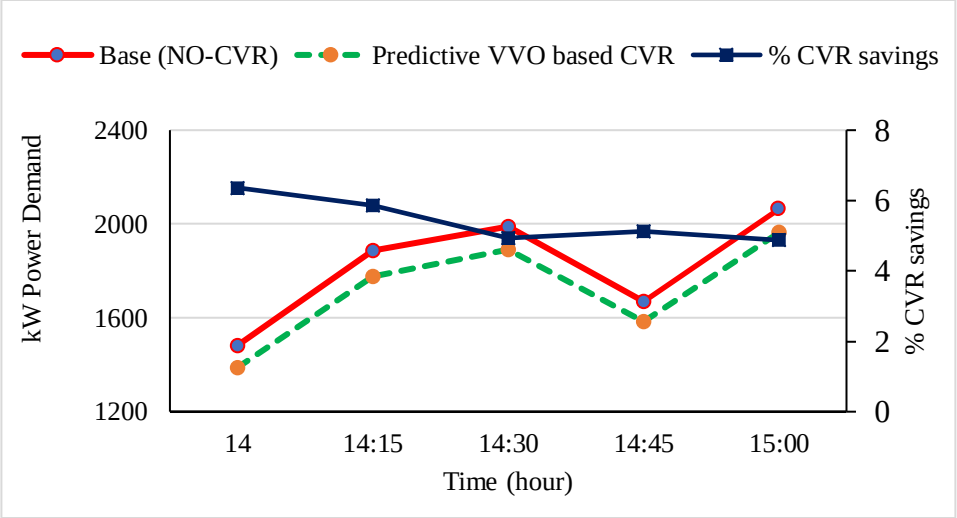

Figure 7.10 Active power demand and percentage CVR power savings

Table 7.2 VVO Set Points Change

Device/Time	14:00–14:15	14:15–14:30	14:30–14:45	14:45–15:00
OLTC	*NC, (Hourly)			
CB	NC, (Hourly)			
AVRs	NC	1	2	NC
SI Q step	NC	NC	1	NC

*NC – No change required, already at the optimal state

7.6.4.2 *Illustration under FTSC: Emergency Action*

During the occurrence of unpredicted events in fast timescale, the emergency action is executed in a real-time control layer by a local adaptive droop controller autonomously. To illustrate the effect of the developed adaptive control *algorithm 3*, two subcases of local droop control with unpredicted external disturbances have been examined as under.

- *Sudden cloud transient Appearance*

An arbitrary instantaneous point between time intervals from 14:00 to 14:15 is selected. The load demand is 1.0 p.u., and solar irradiation is 0.81 kW/m^2 at this instant. During this time span, the lowest voltage profile at Node 114a becomes vulnerable to any reduction in kilowatt power. The status of the volt/VAR regulation devices—OLTC, AVRs, and capacitor banks—remains the same as in the STSC determined by *Algorithm 2*. The solar irradiation reduces from 0.81 to 0.1 kW/m^2 because of the sudden appearance of cloud transients. Accordingly, the reduction in PV power production is reported. The decrease in active PV power injection results in a decrease in the voltage profile and system and might violate the lowest feeder voltage limit. In this study, a similar scenario is observed. The lower voltage limit (0.95 p.u.) is violated as the sudden drop in solar irradiation is reported. Figure 7.11 shows the lowest voltage profile at Node 114a without control, with conventional droop control and adaptive drop control in real-time. This figure shows that the violation of the lower voltage limit occurs when the PV inverters do not have autonomous control and even during the operation of conventional drop controller. This study employs autonomous control using the adaptive droop-based controller in real-time. Figure 7.11 also shows that there no lower voltage limit violation is reported locally when enabling autonomous controls using the proposed two-level adaptive droop controller for better visual comparison. Figure 7.12 shows the additional reactive power compensated by the adaptive droop controllers of PV inverters.

- *Sudden cloud transient Disappearance:*

An arbitrary instantaneous point between time intervals 15:00 to 15:15 is selected. The load demand is 0.40 p.u., and solar irradiation is 0.41 kW/m^2 at this instant due to cloudy weather. The sudden cloud disappearance and solar irradiation vary from 0.41 to 0.8 kW/m^2.

Accordingly, an increase in PV power production is reported. The PV3 power plant located at 104c is most affected and it violates the maximum voltage limit (1.02 p.u) at point of connection. Other PV power plant voltage remains within range. Figure 7.13 shows the comparative analysis of voltage profiles.

Figure 7.11. Lowest feeder voltage profile at Node 114a without control, conventional droop controller, and adaptive droop controllers.

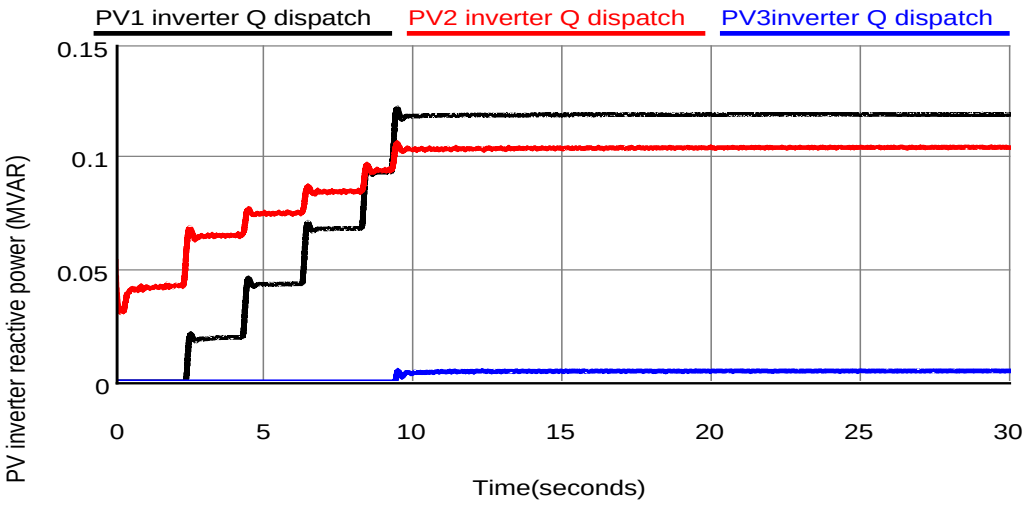

Figure 7.12 Per phase additional reactive power compensation from PV inverters

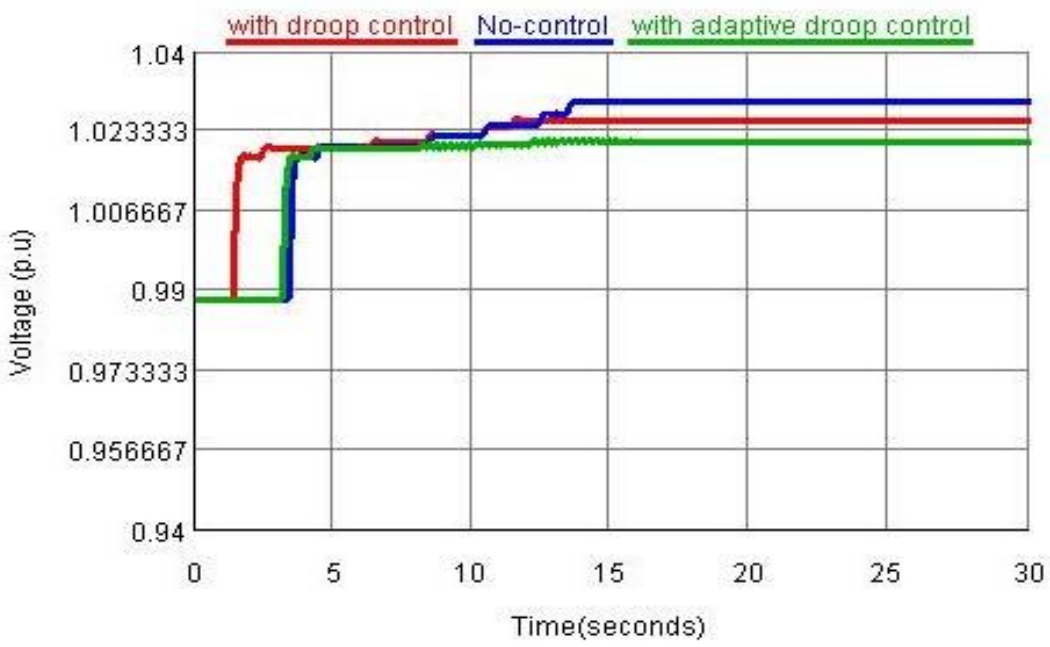

Figure 7.13 Voltage at PV3 node No control,with the conventional droop and with adaptive droop control

7.7 Conclusion

This chapter investigated the impact of CVR on energy savings in the presence of high penetrations of PV with multiple timescale control operation. An event-driven predictive control has been employed to handle the uncertainties and disturbances in PV power generation and loads under aggregated as well as the autonomous control mode. The adaptive droop control method has been used for autonomous control to mitigate the local voltage drop/rise issue during cloud transients' effect in PV active power. The simulation results reveal that the proposed event-driven predictive control method yields better performance than the LDC in terms of voltage fluctuation control and energy savings during CVR operation, even when intermittency occurs in PV power output. Moreover, the developed real-time co-simulation platform validates the effectiveness of the proposed control algorithms. The findings of this investigation are as follows:

- A significant reduction in peak load demand and daily energy demand have been achieved with the proposed method.
- The developed control methodology is proficiently capable of handling the disturbances (uncertainty and intermittency) of the active networks.
- The developed real-time co-simulation platform using the RTDS (distribution mode) could be useful for the study of large-scale practical distribution systems.